Altitude distribution of stratospheric NO3. 1. Observations of NO3 and related species

Jean-Pierre Naudet, Pierre Rigaud, Michel Pirre, Daniel Huguenin

JOURNAL OF GEOPHYSICAL RESEARCH, VOL. 94, NO. D5, PAGES 6374–6382, MAY 20, 1989

Altitude Distribution of Stratospheric NO_3 1. Observations of NO_3 and Related Species

JEAN-PIERRE NAUDET, PIERRE RIGAUD, AND MICHEL PIRRE

Laboratoire de Physique et Chimie de l'Environnement, CNRS, Orléans, France

DANIEL HUGUENIN

Observatoire de Genève, Sauverny, Switzerland

Five balloon-borne observations of the vertical profile of stratospheric NO_3 and ozone were performed between 1981 and 1985 by using the star and planet occultation technique at 662 nm. During the last two flights, NO_2 was also measured by the same technique at 440 nm. The latest available laboratory determination of the 662-nm absorption cross section of NO_3 has been used for the data analysis. This gives NO_3 concentrations that are about a factor of 2 lower than those previously reported. The concentration of NO_3 increases with altitude, from about 1×10^7 molecules cm^{-3} around 22 km, to 2×10^7 molecules cm^{-3} at 38 km in September. A maximum value of 4×10^7 molecules cm^{-3} was observed at 38 km in May 1982. Ozone and NO_2 results obtained from the same flights as NO_3 are also presented. A companion paper provides details on the comparison between observed and modeled NO_3 vertical profiles.

1. INTRODUCTION

Stratospheric NO_3 is produced at night by the reaction of ozone with NO_2 and leads to N_2O_5 formation through its reaction with NO_2. During the day the concentration of stratospheric NO_3 is expected to be very small because of the rapid photolysis of this molecule by sunlight; therefore measurements have to be made at night.

NO_3 was first detected from the ground by *Noxon et al.* [1978], using its absorption near 662 nm in the lunar spectrum. The total column amount of NO_3 was continuously measured for 5 years by *Norton and Noxon* [1986] at different locations in the northern hemisphere. In this set of observations, NO_3 abundances vary from about 10^{14} molecules cm^{-2} to below the detection limit of 10^{13} molecules cm^{-2}. Recently, *Sanders et al.* [1987] measured a total column of about 2×10^{13} molecules cm^{-2} in Antarctica during the nights of September, using the same optical method as Noxon. Other ground-based observations concerned tropospheric NO_3, which can reach large concentrations in polluted environments [*Noxon et al.*, 1980; *Platt et al.*, 1981]. Furthermore, an in situ observation using a balloon-borne cryosampler was reported by *Helten et al.* [1985].

The vertical profile of stratospheric NO_3 has been measured, simultaneously with ozone, by star and planet occultations in the visible spectrum near 662 nm. Results from four balloon flights have already been reported [*Naudet et al.*, 1981, 1985; *Rigaud et al.*, 1983]. The latest observation was part of the MAP/GLOBUS intercomparison campaign in September 1983 [*Pommereau et al.*, 1987; *Simon et al.*, 1987]. Recently, a new balloon-borne observation was made during the second MAP/GLOBUS campaign in September 1985, and this paper presents the full set of NO_3 data deduced from these observations. The accuracy of the data will be discussed with respect to the absorption cross section of NO_3. In particular, new laboratory determinations of this cross section lead to a correction for our previously published NO_3 results, mentioned earlier.

Since NO_3 is formed by reaction of ozone with NO_2, it was decided to measure the vertical profile of NO_2 in addition of NO_3 and ozone during both MAP/GLOBUS balloon flights in September 1983 and 1985. The star occultation technique was used, as for previous NO_2 measurements [*Naudet et al.*, 1984], and the NO_2 results from both observations are presented in this paper.

The rate constant for the formation of NO_3 is so sensitive to temperature that it is of crucial importance to know the temperature as a function of altitude, in order to understand better stratospheric NO_3 chemistry. Fortunately, temperature data were available from meteorologic radiosoundings, from satellites, and from lidar at times and locations close to each balloon flight. Therefore this paper presents a useful set of data for theoretic calculations of NO_3. Such calculations and comparison between modeled and observed NO_3 profiles will be discussed in detail in a companion paper [*Pirre et al.*, this issue].

2. OBSERVATIONS

The experimental technique was described in detail by *Rigaud et al.*, [1983]. Briefly put, the intensity of a rising or setting bright star or planet is recorded from a stabilized balloon platform, so as to determine the atmospheric transmission on optical paths tangential to the atmospheric layers. Following this, a mathematical inversion process yields the distribution of the absorbing constituents as a function of altitude. This occultation technique is extremely powerful in detecting minor atmospheric constituents, as the length of the optical path through the atmosphere (several hundreds of kilometers) compensates for the low absorption of the constituents.

The instrument was composed of a 20-cm Cassegrain telescope, a double-grating Jobin-Yvon monochromator

Paper 88JD03856.
0148-0227/89/88JD-03856$05.00

TABLE 1. Flight Characteristics

	Sept. 12, 1980	Sept. 18, 1981	May 3, 1982	Sept. 14, 1983		Sept. 24, 1985	
Balloon height, km	38.8	38.8	39.5	38.9	38.8	39.5	39.5
Light source	Venus	Arcturus	Venus	Sirius	Venus	Sirius	Venus
Reference zenith angle	71.3°	81.4°	85.4°	86.0°	81.3°	81.7°	78.2°
Time at which Z=90°, UT	0150	2142	0320	0217	0329	0137	0318
Spectral range, nm	647–672	647–672	647–672	427–452	647–672	427–452	647–672
Objective	NO_3, O_3	NO_3, O_3	NO_3, O_3	NO_2	NO_3, O_3	NO_2	NO_3, O_3

controlled by a stepping motor, and a photomultiplier used in the photon-counting mode. A spectral span of 25 nm was swept cyclically in 0.2-nm increments in 6.4 s, with a final resolution of 1 nm.

Table 1 lists the balloon flights, which all took place from the French Centre National d'Etudes Spatiales (CNES) launching base of Aire-sur-l'Adour (43°42'N, 0°15'W). All measurements were made in September, apart from a springtime observation in May 1982. In 1983 and 1985 flights were part of the first and second MAP/GLOBUS intercomparison campaigns. Float altitudes were around 38–40 km, and balloons remained at geographic coordinates close to the launching base. The planet Venus and the star Arcturus were used as light sources to measure, simultaneously, absorption by NO_3 and ozone in the spectral range 647–672 nm, where NO_3 absorption has a strong maximum near 662 nm and ozone absorption decreases with wavelength. In September 1983 and 1985, two occultations were successively recorded during the same flight. The spectrometer was first pointed at the rising star Sirius to measure the absorption by NO_2 between 427 and 452 nm, where the NO_2 absorption cross section displays a series of maxima and minima. Then, the spectrometer was pointed at the rising planet Venus to measure absorption by NO_3 and ozone. These light sources were selected for their brightness, which is strong enough to make observations possible through the large air mass of the atmospheric tangential optical path. Also, their spectra show a smooth continuum, with very few lines that do not interfere with the broad absorption band of NO_2 near 440 nm and NO_3 near 662 nm. The most marked stellar signatures are the H_γ line at 434.0 nm for Sirius and the H_α line at 656.3 nm for Arcturus and Venus. These lines were used as wavelength references for the calibration of observed spectra. For each occultation, Table 1 also gives the lowest zenith angle for which observations were taken and the time corresponding to the observation of the star or planet at a zenith angle of 90°.

3. Data Analysis

More than 500 spectra were recorded during each occultation, over zenith angles symmetrical with regard to 90°. The first stage in data reduction was to filter out the noise due to atmospheric scintillation at zenith angles larger than 92°. A substantial part of it was removed from Venus spectra between 647 and 672 nm by normalizing the spectrometric signal with respect to the broadband signal of the tracking system. Although the same procedure was also applied to Arcturus and Sirius spectra, the signal-to-noise ratio was not improved as much as for Venus spectra because of the zero diameter of stellar sources. Further improvement was obtained by adding up 20–40 consecutive scans, so as to obtain average spectra over a period of 2 min for the planet Venus and 4 min for the stars. After this, the wavelength scale of each spectrum was adjusted to the H_γ (434.0 nm) or H_α (656.3 nm) line of the source spectrum. The atmospheric transmission was then deduced from the ratio of each average spectrum with a reference spectrum of the corresponding star or planet. Although the reference spectrum should be taken above the atmosphere, in practice, the least attenuated spectrum recorded by the balloon-borne spectrometer at $Z \leq 86°$ (Table 1) was used. Therefore the reference spectrum contains a small absorption due to the residual atmosphere above the balloon. Correction for this will be discussed later. When the ratio spectrum was properly obtained, perfect removal of the stellar lines was observed. The only remaining features are due to absorption by NO_3 and ozone near 662 nm and by NO_2 near 440 nm along the atmospheric optical path. Attenuation by molecular and aerosol scattering is also present in both spectral ranges. Water vapor, which has some weak absorption lines whose spectral characteristics are not well known, was not detected in this experiment.

3.1. *NO_3 and Ozone Absorption Spectra*

In the spectral range 647–672 nm, a synthetic spectrum taking into account the attenuation by molecular scattering and the absorption by NO_3 and ozone was fitted to each experimental spectrum, using a least squares method (Figure 1). The NO_3 absorption has a strong maximum at 662 nm, the O_3 absorption linearly decreases with wavelength, and molecular scattering is decreasing in λ^{-4}. These attenuations were sufficient to explain observations at zenith angles smaller than 94°. For larger angles it was necessary to take into account the attenuation due to aerosol scattering, which may be assumed to be wavelength-independent over the narrow spectral range 647–672 nm. This corresponds to an aerosol size typical of the lower stratosphere after the eruption of El Chichón in April 1982 [*Rosen and Hofmann*,

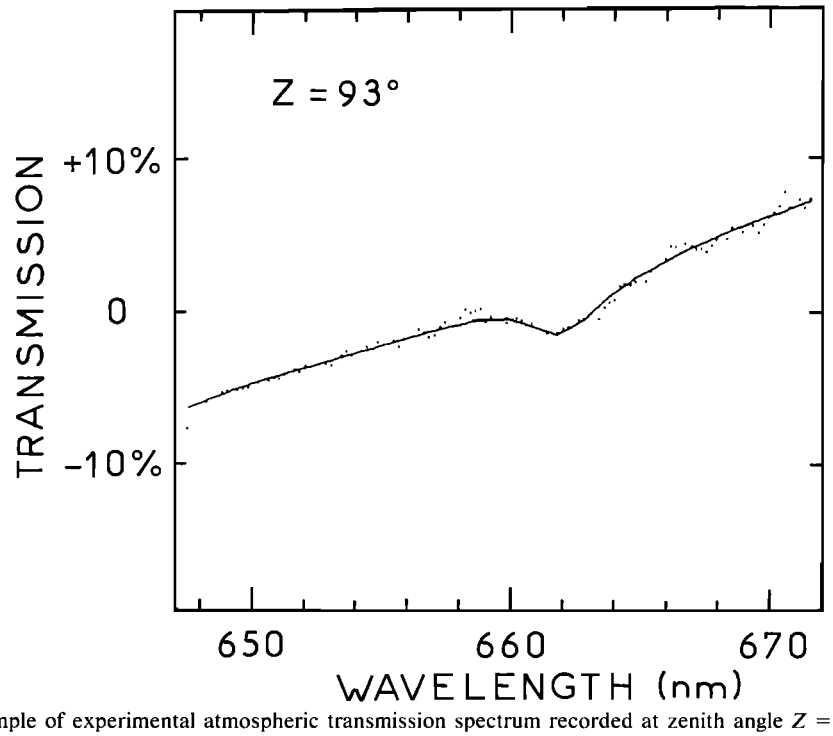

Fig. 1. Sample of experimental atmospheric transmission spectrum recorded at zenith angle $Z = 93°$ during the occultation of Venus in September 1985 (dots), compared to fitted synthetic spectrum taking into account the attenuation by NO_3, ozone, and molecular scattering (solid curve).

1986]. Lower aerosol attenuation was detected before this eruption, and the sensitivity of the determination of ozone and NO_3 amounts to the possible wavelength dependence of this attenuation was found to be neglectable in the altitude range considered here (above 20 km). Molecular scattering was calculated using the air mass tabulated by *Link and Neuzil* [1969] and the extinction coefficient from *Nicolet* [1984]. NO_3 and ozone column densities and aerosol optical depth along the path length were regressed, so as to minimize the deviation between the computed and the experimental spectrum.

Figure 2 shows the contribution of ozone, NO_3, and scattering by molecules and aerosol to the total optical depth at 662 nm along a tangential path, as a function of the zenith angle and for the observation of September 1983. Figure 2 is typical of all observations reported in this paper, except for the aerosol optical depth, which differs from one observation to another. The largest aerosol amount was observed during the flight of September 1983, as a result of the eruption of El Chichón in April 1982. Aerosol observations will be discussed at a later date. Absorption by NO_3 is detected at zenith angles smaller than 94°, while ozone absorption dominates over other attenuations. This makes the determination of ozone column density quite accurate. For example, the upper limit error for molecular scattering calculation is 20% and results from different sources of systematic error, including geographic localization by radar, balloon height, and the atmospheric density profile use for air mass calculation. This error would lead to a systematic error of less than 3% for the determination of the ozone column density. On the other hand, the profile of NO_3 absorption, which strongly differs from those of other attenuations, makes the determination of the NO_3 column density independent of ozone absorption and molecular scattering attenuation. Therefore the least squares fit of each observed spectrum yields a unique combination of NO_3 and ozone column densities.

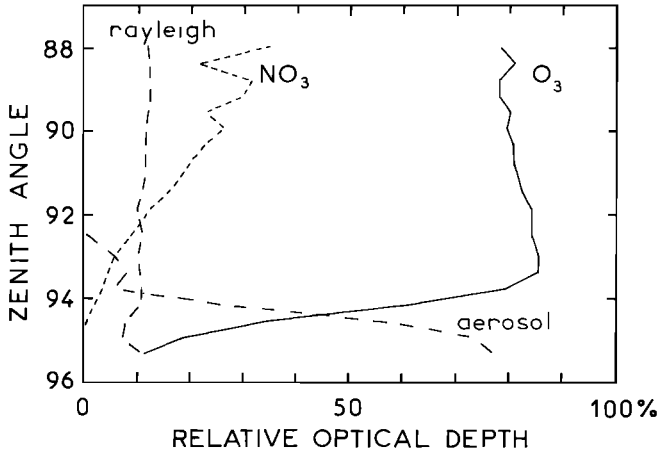

Fig. 2. Relative optical depth of NO_3, ozone, and scattering by molecules and aerosol along optical path versus zenith angle, as observed at 662 nm during the occultation of Venus in September 1983.

The least squares fit to the spectrum provides a statistical measure of the precision with which all spectral features can be fitted. As an example, for the observation of September 1985, the standard deviation was less than 2% and within 5–10% for ozone and NO_3 column densities, respectively. Other errors are systematic and arise from the absolute value of absorption cross sections.

Laboratory determinations of the ozone absorption cross section are coherent within about 5% [*Vigroux*, 1953; *Inn and Tanaka*, 1953; *Griggs*, 1968]. Values used in this work are the result of the average of these three studies. Further-

TABLE 2. NO_3 Absorption Cross Section at 662 nm

	Temperature, K			
	298	240	230	220
Ravishankara and Mauldin [1986]	1.90×10^{-17}	2.31×10^{-17}		2.71×10^{-17}
Sander [1986]	2.28×10^{-17}		2.67×10^{-17}	
Cantrell et al. [1987]	2.06×10^{-17}		temperature independent	

Cross sections are in units of square centimeters per molecule.

more, this cross section is independent of temperature and pressure [*Humphrey and Badger*, 1947].

For previous determinations of NO_3 data [*Naudet et al.*, 1985], we used the shape of the NO_3 absorption band as given by *Graham and Johnston* [1978], corrected by a factor of 0.7 so that the value of the maximum cross section was equal to the determination by *Mitchell et al.* [1980]: 1.21×10^{-17} cm^2 at 662 nm. However, new laboratory measurements of the NO_3 absorption cross section as a function of wavelength have been reported by *Ravishankara and Wine* [1983], *Cox et al.* [1984], *Burrows et al.* [1985], *Sander* [1986], *Ravishankara and Mauldin* [1986], and *Cantrell et al.* [1987]. Values obtained for a temperature of 298 K range from 1.21×10^{-17} cm^2 [*Marinelli et al.*, 1982] to 2.28×10^{-17} cm^2 [*Sander*, 1986]. Two of these studies [*Sander*, 1986; *Ravishankara and Mauldin*, 1986], indicate that the absorption cross section increases with decreasing temperature. This was not confirmed by *Cantrell et al.* [1987]. In the present work, we have adopted a temperature-independent value of $2.08 \pm 0.3 \times 10^{-17}$ cm^2, as recommended by *Cantrell et al.* [1987], which is the result of the average of the three most recent studies at 298 K (Table 2).

3.2. *NO_2 Absorption Spectra*

Absorption by NO_2 between 427 and 452 nm represents a few percent of the total attenuation, which is mainly due to molecular scattering. In addition, ozone has some weak absorption bands at these wavelengths. The NO_2 column density along the optical path was deduced from each transmission spectrum by using a method similar to that described by *McMahon and Simmons* [1980]. Each spectrum was first corrected for the attenuation by molecular scattering, which was calculated in the same manner as for NO_3 and ozone absorption spectra. A small correction for ozone absorption was also applied, using the cross section from *Vigroux* [1953] and the ozone vertical profile published by *Krueger and Minzner* [1976]. A simulated calculation has shown that neglecting ozone absorption within the wavelength range considered here leads to an error of about 5% in the determination of NO_2 column density. The next step was to eliminate from each corrected spectrum the attenuation due to aerosol scattering, which is almost independent of wavelength, and also to remove the effect of a possible uncertainty smaller than 20% in the calculation of the molecular scattering correction. This was made by fitting a straight line to each corrected spectrum, using the least squares method; then the deviation from this line was regressed against a synthetic spectrum of NO_2 absorption, also expressed as a deviation from the best fit line.

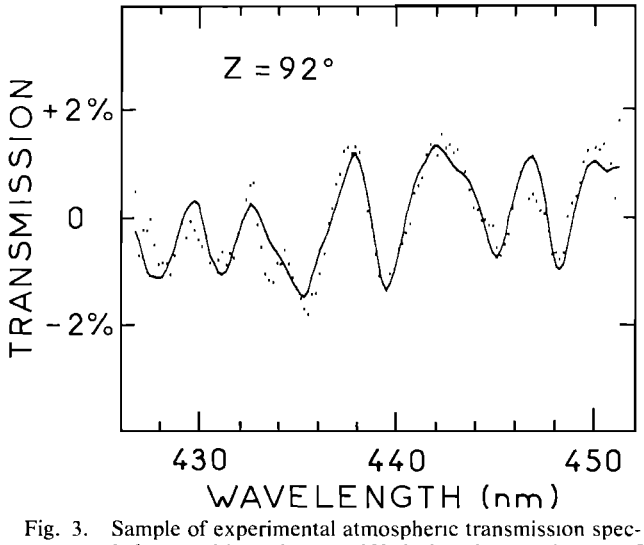

Fig. 3. Sample of experimental atmospheric transmission spectrum recorded at zenith angle $Z = 92°$ during the occultation of Sirius in September 1985 (dots), compared to fitted synthetic spectrum taking into account the attenuation by NO_2, ozone, and molecular scattering (solid curve).

Figure 3 shows an example of comparison between observed and calculated spectra, taking into account the attenuation by molecular scattering and the absorption by NO_2 and ozone. The spectrum of NO_2 exhibits six strong absorption bands at 427.8, 431.0, 435.2, 439.4, 445.0 and 448.2 nm. The standard deviation is about 20% for the NO_2 column density, not including the uncertainty on the absolute value of the NO_2 absorption cross section. This cross section was deduced from laboratory measurements, using the same spectrometer as in flight and glass cells with known amounts of NO_2, in the range of optical depths encountered during the flights. Accuracy is better than 10% [*Naudet et al.*, 1984]. An additional systematic error of about 10% may arise from the cross section temperature dependence, which is not well known [*Leroy et al.*, 1987].

3.3. *Inversion*

The altitude distribution of ozone, NO_2, and NO_3 was derived from their corresponding column densities by using a tangent ray inversion technique. The atmosphere was represented by a spherical layer model, assuming that all of the species were uniformly distributed within each layer. For each species the set of column densities $N(Z)$ obtained for discrete values of zenith angle Z can be expressed as

$$N(Z) = \sum_{j \leq k} a_j(Z) n_j + \sum_{j > k} a_j(Z) n_j - \sum_{j > k} a_j(Z_0) n_j \qquad (1)$$

where $a_j(Z)$ and n_j are the length of optical path and the concentration within the jth layer, respectively. The first right-hand term in (1) represents the sum of the contributions

from the tangent layer up the balloon layer k; the second term is the contribution from the layers above the balloon; the last term is a correction term that represents the residual column density for the reference spectrum observed from the balloon, at zenith angle Z_0. The set of equations (1) can be solved for n_j using either a least squares algorithm or a nonlinear iterative method, as described by *Twomey* [1975]. However, it is well known that the geometry of observations by the tangent ray technique prevents an accurate retrieval of the altitude distribution above the balloon. We avoided this difficulty by making the following hypothesis.

Ozone and NO_2 concentrations were assumed to decrease exponentially above the balloon with a given scale height H. Such behavior is expected from observations as well as from model calculations [e.g., *World Meteorological Organization (WMO)*, 1985]. By using this assumption the contribution of the layers above the balloon can be expressed as a function of the concentration n_k in the balloon layer. Equation (1) becomes

$$N(Z) = \sum_{j \leq k} a_j(Z) n_j + [S(Z, H) - S(Z_0, H)] H n_k \qquad (2)$$

where $S(Z, H)$ and $S(Z_0, H)$ are computed Chapman functions, which mainly depend on zenith angle and scale height. The scale height can be estimated from column densities observed at zenith angles lower than 90°. These may be expressed as

$$N(Z < 90°) = [S(Z, H) - S(Z_0, H)] H n_k \qquad (3)$$

The set of equations (3) was solved for n_k with, successively, different values of H, until calculated and observed column densities agreed within error range. As an example, the scale height range that fits the observation of September 1985 was $3.5 \leq H \leq 4.5$ km for ozone and $6 \leq H \leq 11$ km for NO_2. Following this, the concentration was computed in each layer, using a least squares algorithm with, successively, the minimum and maximum value of scale heights. It was noted that only the concentration at balloon level is sensitive to the choice of H, whereas all concentrations at lower altitudes remain practically unchanged owing to the inversion process geometry. The random error arising from the signal-to-noise ratio was calculated from the covariance matrix.

On the basis of photochemical models, the NO_3 concentration is expected to increase above the balloon up to about 40 km altitude [*Naudet et al.*, 1981; *WMO*, 1981]. As no experimental data are available for heights above 38–39 km, modeled profiles from *Pirre et al.* [this issue] were used to correct each observed NO_3 column density from the residual NO_3 amount in the reference spectrum (last term of equation (1)). This correction appears as a circular procedure, since balloon data will be used to validate the model; its effect on NO_3 retrieval will be discussed later. Then the set of equations (1) was solved for n_j by iterations. The method consisted of starting with a first guess of n_j and repeatedly proceeding through each measurement until calculated and observed column densities agreed within error range. At each step all concentrations above the balloon were modified by the same factor, so that the shape of the top profile remained unchanged. The procedure was repeated with different initial guesses of n_j. The standard deviation to the mean of the results gives an estimation of the random error.

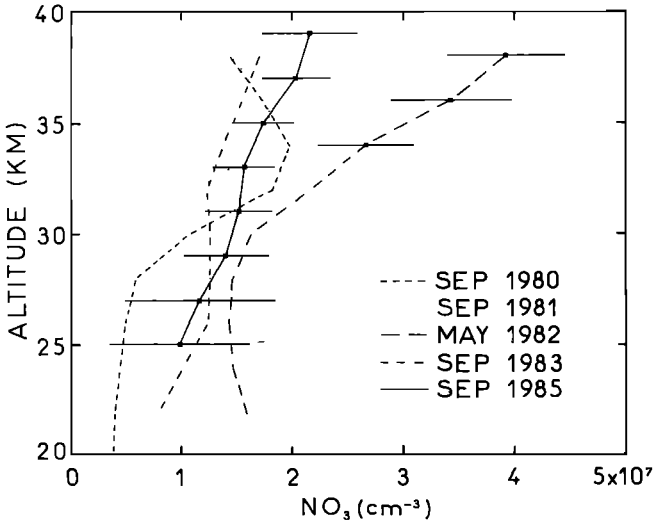

Fig. 4. Altitude distribution of NO_3 observed at night.

4. Results

Figures 4–6 give the altitude distribution of NO_3, ozone, and NO_2, deduced from the observations listed in Table 1. Numerical values are tabulated in Tables 3–7. Altitude was deduced from pressure using the U.S. Standard Atmosphere (1976). The horizontal bars represent the uncertainty arising from the column density dispersion, from the inversion process, and from the uncertainty on the residual absorption above the balloon. Uncertainty arising from the absolute value of cross sections is 5% for ozone, 18% for NO_3, and 10% for NO_2. The uncertainty on balloon heights, which is less than 0.5 km, leads to an uncertainty of the same magnitude on altitude scales. The latter translates to an uncertainty on concentrations that is proportional to the gradient of concentration with respect to altitude.

The possible temperature dependence of NO_2 and NO_3 cross sections was not considered here. According to the laboratory data on NO_2 and NO_3 cross sections from *Leroy et al.* [1987] and *Ravishankara and Mauldin* [1986], respectively, this dependence would decrease the concentration of NO_2 by about 10% at 30 km and that of NO_3 by about 30% at 20 km.

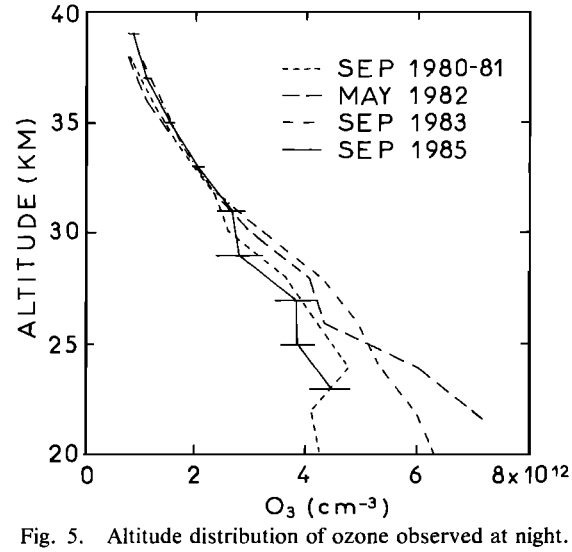

Fig. 5. Altitude distribution of ozone observed at night.

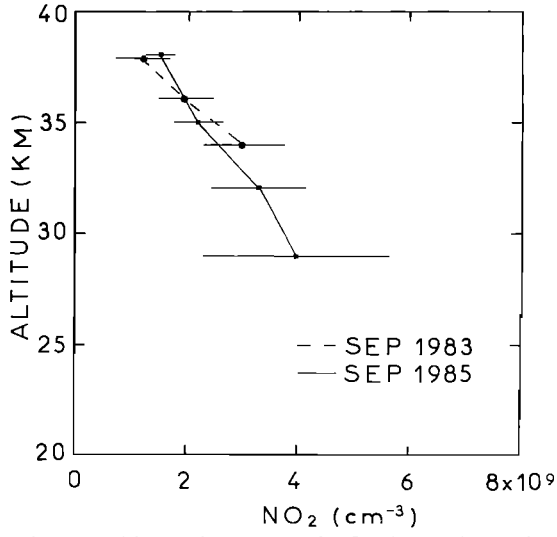

Fig. 6. Altitude distribution of NO_2 observed at night.

It should also be remembered that NO_3 was observed simultaneously with ozone, whereas NO_2 was observed about 1–2 hours before NO_3 and ozone.

4.1. NO_3

Concentrations plotted in Figure 4 are lower by a factor of about 1.72 than those previously published by *Naudet et al.* [1981, 1985], and *Rigaud et al.*, [1983]. This results from the difference between the value of the maximum NO_3 cross section from *Cantrell et al.* [1987] used in the present work 2.08×10^{-17} cm^2, and that from *Marinelli et al.* [1982] used in our previous work, 1.21×10^{-17} cm^2.

Above 30 km, NO_3 concentrations taken in September are close to each other, whereas higher values were obtained in May 1982. At lower altitudes, low values were obtained in September 1980.

The observation of May 1982 indicates that the maximum NO_3 concentration must be above 39 km. NO_3 concentrations were corrected from the NO_3 amount above the balloon in the following manner. The zenith angle of the reference spectrum for this observation is 86°. The corresponding column density of NO_3 was calculated, using a modeled profile, and introduced in the inversion process as explained earlier. This correction enhanced the NO_3 concentration at 39 km by about 30%. For comparison, the correction of other profiles is less than 12% at 38–39 km, because of the smaller amount of NO_3 above the balloon and the lower zenith angle of the reference spectrum (see Table 1). In all cases, the effect of this correction rapidly decreases as altitude decreases because of the geometry of the inversion process. Note that these corrections are much smaller than the difference at 38–39 km between the NO_3 concentrations observed in May 1982 and those observed in September. This gives confidence in the seasonal variation seen in Figure 4.

TABLE 3. Nighttime Concentrations of Ozone and NO_3 Observed September 12, 1980

Altitude, km	O_3, $\times 10^{12}$ cm^{-3}	NO_3, $\times 10^7$ cm^{-3}
38	0.79 ± 0.10	1.45 ± 0.32
36	1.30 ± 0.08	1.74 ± 0.23
34	1.60 ± 0.09	1.98 ± 0.24
32	2.31 ± 0.18	1.83 ± 0.15
30	2.62 ± 0.25	1.09 ± 0.31
28	3.62 ± 0.29	0.60 ± 0.31
26	4.20 ± 0.28	0.50 ± 0.29
24	4.78 ± 0.23	0.45 ± 0.27
22	4.10 ± 0.28	0.41 ± 0.25
20	4.26 ± 0.22	0.39 ± 0.25

TABLE 4. Nighttime Concentrations of Ozone and NO_3 Observed September 18, 1981

Altitude, km	O_3, $\times 10^{12}$ cm^{-3}	NO_3, $\times 10^7$ cm^{-3}
38	0.79 ± 0.10	1.45 ± 0.48
36	1.30 ± 0.08	1.80 ± 0.52
34	1.60 ± 0.09	1.80 ± 0.47
32	2.31 ± 0.18	1.15 ± 0.48

Other NO_3 observations are total atmospheric columns, as reported by *Noxon et al.* [1978], *Norton and Noxon* [1986] and *Sanders et al.* [1987]. The observations from *Norton and Noxon* [1986] indicate that the total column at mid-latitudes strongly depends on season, with values ranging from 10^{13} molecules cm^{-2} in winter to 10^{14} molecules cm^{-2} in May. Comparison of these with balloon observations would need to turn vertical profiles into total columns. But, the contribution from heights above the balloon, which may be important because the maximum NO_3 concentration is located at balloon height or at even higher altitudes, cannot be accurately deduced using the occultation technique. Also, because of the limited duration of each flight, the range of zenith angles of observation of the planet Venus was not large enough to permit an accurate determination of the column of NO_3 above the balloon. Nevertheless, total columns were estimated as follows. For each flight, the vertical profile observed below 38–39 km was extrapolated up to 50 km, using the corresponding modeled profile from *Pirre et al.* [this issue]. The integrated column abundance of the extrapolated profile was then calculated. Results are 3.4, 7.6, 3.6, and 3.8×10^{13} molecules cm^{-2} for September 1980, May 1982, September 1983, and September 1985, respectively. These values are consistent with those observed by *Norton and Noxon* [1986]. In particular, balloon observations that indicate NO_3 concentrations larger in May than in September corroborate the seasonal variation of NO_3. Further comparison would need to take into account ozone and temperature, as pointed out by *Pirre et al.* [this issue].

Norton and Noxon [1986] have reported that at all times of the year, low NO_3 values seem to be associated with air that had previously been at high latitudes. Stratospheric air trajectory analyses, performed for the time and location of each balloon flight, show that the air had reached about 55°N in September 1980 and about 65°N in September 1981 [*Norton and Noxon*, 1986]. For the observation of May 1982, which shows larger concentrations of NO_3, air remained at lower latitude (J. F. Noxon, private communication, 1984). This would support the previously mentioned relation between the abundance of stratospheric NO_3 and the past history of the air mass. However during the MAP/GLOBUS campaign of 1983, which showed low NO_3, no fast transport from high or low latitudes was inferred from the meteorological data [*Langematz et al.*, 1987]. Even so, the results of only five balloon flights performed at the same latitude do

TABLE 5. Nighttime Concentrations of Ozone and NO_3 Observed May 3, 1982

Altitude, km	O_3, $\times 10^{12}$ cm^{-3}	NO_3, $\times 10^7$ cm^{-3}
38	0.75 ± 0.03	3.92 ± 0.53
36	1.10 ± 0.05	3.43 ± 0.54
34	1.69 ± 0.07	2.66 ± 0.43
32	2.26 ± 0.09	2.18 ± 0.44
30	3.02 ± 0.12	1.64 ± 0.49
28	4.03 ± 0.14	1.47 ± 0.51
26	4.34 ± 0.16	1.44 ± 0.57
24	6.00 ± 0.21	1.47 ± 0.71
22	7.02 ± 0.41	1.59 ± 0.99

not provide a statistical basis permitting a detailed study of the relation between dynamics and chemistry.

As already mentioned, the formation of NO_3 is strongly temperature-dependent. Temperature was measured by a standard thermistor on board the gondola. But, at low pressure the thermal equilibrium of the thermistor mainly depends on radiation processes, rather than on conduction. This led to an underestimation of the temperature measured above about 30 km during the period of slow ascent and at float altitude. In the present work we have used temperature data from the National Meteorological Center (NMC) and from other MAP/GLOBUS observations, which are available for times and locations close to each balloon flight. The temperature dependence of NO_3 concentration is explained by *Pirre et al.* [this issue], who show that a difference of 10 K between May and September explains quite well the large values of NO_3 observed in May 1982.

4.2. *Ozone*

Only four profiles have been plotted on Figure 5 because the concentrations observed in September 1980 and September 1981 were identical within error range. For this reason, it was sufficient to plot the mean of both profiles in Figure 5.

Ozone concentrations were lower in September 1980/1981 and September 1985 than in May 1982. This is likely related to the seasonal variation of ozone in the stratosphere, since at middle and high northern latitudes, ozone reaches a maximum at the end of March and then decreases until October [e.g. *Brasseur and Solomon*, 1984].

Larger values were also obtained in September 1983 during the first MAP/GLOBUS campaign. Comparison with other observations performed during the same campaign have been discussed by *Simon et al.* [1987] and *Matthews et al.* [1987]. These authors note, in particular, that ozone concentrations obtained by planet occultation on September 14 were systematically larger than those obtained by in situ techniques a few hours later and on September 28. *Simon et al.* [1987] suggest that the large amount of aerosol present in the stratosphere at this time may prevent an accurate determination of ozone below 30 km, whereas *Matthews et al.* [1987] suggest that the absorption cross-section data could be the possible cause for the discrepancy. Also, *Offermann* [1987] shows that a wave structure present in the atmosphere during the whole campaign may have induced a perturbation in ozone concentrations.

However, D. E. Robbins (private communication, 1988) recently compared the ozone results of the 1985 MAP/GLOBUS campaign. As we have used the same instrument and the same method (venus occultation) as for MAP/GLOBUS 1983, it is interesting to report that the results from this occultation agree within 10% with other results from in situ and remote experiments that measured ozone in the same stratospheric air mass. Therefore the discrepancy of September 1983 does not result from the limb-scanning technique.

The total ozone maps available from the Dobson network indicate that atmospheric ozone was far from uniformly distributed over Europe during MAP/GLOBUS 1983 [*Attmannspacher et al.*, 1987]. For example, the total ozone measured at Uccle, Belgium (51°N, 4°W), decreased from 365 to 255 m (atm cm)$_{STP}$ between September 12 and 28, 1983 (D. De Muer, private communication, 1985). This strongly suggests that the air mass sampled by the Venus occultation technique on September 14 was different from that sampled by the in situ technique on September 28. Therefore the results from the two techniques cannot be directly compared.

The ozone profiles taken by the lidar at the Zugspitze station in Germany (47.5°N, 11°E) on September 13, 14, and 15, show considerable wave activity [*Werner et al.*, 1985]. On the other hand, planet occultation measurement involves optical paths through the atmosphere that are several hundred kilometers long. During the flight of September 14, the spectrometer was pointed eastward at the rising Venus and the balloon trajectory was about east. By comparison, the balloon trajectory of the in situ experiment flight, made 7 hours later, was slightly shifted to the north. Therefore optical paths involved in the planet occulation have never overlapped the trajectory of the in situ experiment flight. All these points need to be carefully considered in comparing both observations, even though these observations were performed the same day, with a time lag of only 7 hours. This would need a three-dimensional ozone picture, which will be the subject of future work.

4.3. *NO_2*

The observations of NO_2, presented in Figure 6, were taken during the first and second MAP/GLOBUS intercomparison campaigns of September 1983 and September 1985. Both profiles are almost identical, although the second observation was made 2 years later. Considering the high seasonal and diurnal variability of stratospheric NO_2, it should be noted that both observations are representative of the same season and of local time close to midnight. During the nights of September, NO_2 is expected to represent the

TABLE 6. Nighttime Concentrations of Ozone, NO_3, and NO_2 Observed September 14, 1983

Altitude, km	O_3, $\times 10^{12}$ cm^{-3}	NO_3, $\times 10^7$ cm^{-3}	NO_2, $\times 10^9$ cm^{-3}
38	0.96 ± 0.09	1.71 ± 0.41	1.17 ± 0.49
36	1.37 ± 0.06	1.56 ± 0.22	1.96 ± 0.50
34	1.75 ± 0.07	1.39 ± 0.18	3.03 ± 0.72
32	2.31 ± 0.08	1.24 ± 0.22	
30	3.25 ± 0.11	1.27 ± 0.19	
28	4.28 ± 0.14	1.27 ± 0.19	
26	4.92 ± 0.22	1.25 ± 0.26	
24	5.34 ± 0.27	1.03 ± 0.39	
22	5.97 ± 0.33	0.81 ± 0.49	
20	6.34 ± 0.42		

TABLE 7. Nighttime Concentrations of Ozone, NO_3, and NO_2 Observed September 24, 1985

Altitude, km	O_3, $\times 10^{12}$ cm^{-3}	NO_3, $\times 10^7$ cm^{-3}	NO_2, $\times 10^9$ cm^{-3}
39	0.85 ± 0.08	2.16 ± 0.43	
38			1.51 ± 0.26
37	1.11 ± 0.06	2.04 ± 0.31	
35	1.53 ± 0.08	1.75 ± 0.26	2.20 ± 0.45
33	2.04 ± 0.11	1.57 ± 0.28	
32			3.29 ± 0.85
31	2.66 ± 0.25	1.52 ± 0.30	
29	2.80 ± 0.42	1.41 ± 0.39	3.98 ± 1.67
27	3.82 ± 0.39	1.17 ± 0.68	
25	3.86 ± 0.31	0.99 ± 0 63	
23	4.46 ± 0.35		

major fraction of total odd nitrogen NO_y in the mid-latitude stratosphere [*Pirre et al.*, this issue]. Therefore Figure 6 suggests that NO_y abundance was similar in September 1983 and September 1985.

Comparisons of the profile of September 1983 with other observations and model calculations have already been presented [*Pommereau et al.*, 1987; *Brasseur et al.*, 1987]. Discussion of the profile of September 1985 within the frame of the second MAP/GLOBUS campaign will be presented in a later paper.

5. Conclusion

This paper presents an important set of vertical profiles of stratospheric NO_3. Results were deduced from balloon-borne observations of star and planet occultations at 662 nm. The latest available laboratory determination of the absorption cross section of NO_3 has been used in this work, which makes NO_3 concentrations a factor of 2 lower than those previously reported. An uncertainty still remains, as the most recent laboratory studies have not clearly established whether the NO_3 cross section at 662 nm is temperature-dependent. Observations show that the maximum NO_3 concentration is larger and located at a higher altitude in May than in September. The vertical profiles of ozone measured simultaneously with NO_3 and of NO_2 measured around 440 nm are also reported. This point is of significance in testing atmospheric models, as ozone, NO_2, and NO_3 are partners in photochemical reactions. Comparison of these observations with model calculations is discussed in a companion paper [*Pirre et al.*, this issue].

Acknowledgments. We wish to express our gratitude to the French Space Agency (CNES) and to the Swiss Science Foundation for their constant support of this project.

References

Attmannspacher, W., et al., Ozonesonde and Dobson spectrometer data obtained during the MAP/GLOBUS 1983 campaign over Western Europe, *BPT Ber. 5/87*, Gesellschaft für Strahlen und Umweltforschung, Munich, 1987.

Brasseur, G., and S. Solomon, *Aeronomy of the Middle Atmosphere*, D. Reidel, Hingham, Mass., 1984.

Brasseur, G., D. Cariolle, A. De Rudder, L. J. Gray, J A. Pyle, E. P. Röth, U. Schmailzl, and D. J. Wuebles, Odd nitrogen during the MAP/GLOBUS 1983 campaign. Theoretical considerations, *Planet. Space Sci.*, *35*, 637, 1987.

Burrows, J. P., G. S. Tyndall, and G. K. Moortgat, Absorption spectrum of NO_3 and kinetics of the reactions of NO_3 with NO_2, Cl, and several stable atmospheric species at 298 K, *J. Phys. Chem.*, *89*, 4848, 1985.

Cantrell, C. A., J. A. Davidson, R. E. Shetter, B. A. Anderson, and J. G. Calvert, The temperature invariance of the NO_3 absorption cross section in the 662 nm region, *J. Phys. Chem.*, *91*, 5858, 1987.

Cox, R. A., R. A. Barton, E. Ljungstrom, and D. W. Stocker, The reactions of Cl and ClO with NO_3 radical, *Chem. Phys. Lett.*, *108*, 228, 1984.

Graham, R. A., and H. S. Johnston, The photochemistry of NO_3 and the kinetics of the N_2O_5-O_3 system, *J. Phys. Chem.*, *82*, 254, 1978.

Griggs, M. J., Absorption coefficients of ozone in the ultraviolet and visible regions, *J. Chem. Phys.*, *49*, 857, 1968.

Helten, M., W. Patz, D. H. Ehhalt, and E. P. Roth, Measurements of nighttime NO_3 and NO_2 in the stratosphere by matrix isolation and ESR spectroscopy, in *Atmospheric Ozone*, edited by C S. Zerefos and A. Ghazi, p. 196, D. Reidel, Hingham, Mass., 1985.

Humphrey, G. L., and R. M. Badger, The absorption spectrum of ozone in the visible, *J. Chem. Phys.*, *15*, 794, 1947.

Inn, E. C. Y., and Y. Tanaka, Absorption coefficient of ozone in the ultraviolet and visible regions, *J. Opt. Soc. Am.*, *43*, 870, 1953.

Krueger, A. J., and R. A. Minzner, A mid-latitude ozone model for the 1976 U.S. Standard Atmosphere, *J. Geophys. Res.*, *81*, 4477, 1976.

Langematz, U., K. Labitzke, and E. Reimer, Synoptic analysis and trajectories during the MAP/GLOBUS campaign 1983, *Planet. Space Sci.*, *35*, 525, 1987.

Leroy, B., P. Rigaud, and E. Hicks, Visible absorption cross sections of NO_2 at 298 K and 235 K, *Ann. Geophys.*, *5A*, 247, 1987.

Link, F., and L. Neuzil, *Tables of Light Trajectories in the Terrestrial Atmosphere*, Herman, Paris, 1969.

Marinelli, W. J., D. M. Swanson, and H. S. Johnston, Absorption cross sections and line shape for the NO_3 (0-0) band, *J. Chem. Phys.*, *76*, 2864, 1982.

Matthews, W. A., et al., General comparison of ozone vertical profiles obtained by various techniques during the 1983 MAP/GLOBUS campaign, *Planet Space Sci.*, *35*, 603, 1987.

McMahon, B. B., and E. L. Simmons, Ground-based measurements of atmospheric NO_2 by differential optical absorption, *Nature*, *287*, 710, 1980.

Mitchell, D. N., R. P. Wayne, P. J. Allen, R. P. Harrisson, and R. J. Twin, Kinetics and photochemistry of NO_3, *J. Chem. Soc. Faraday Trans. 2*, *76*, 785, 1980.

Naudet, J. P., D. Huguenin, P. Rigaud, and D. Cariolle, Stratospheric observation of NO_3 and its experimental and theoretical distribution between 20 and 40 km, *Planet. Space Sci.*, *29*, 707, 1981.

Naudet, J. P., P. Rigaud, and D. Huguenin, Stratospheric NO_2 at night from balloons, *J. Geophys. Res.*, *89*, 2583, 1984.

Naudet, J. P., P. Rigaud, and D. Huguenin, Variabilité temporelle du NO_3 stratospherique, in *Atmospheric Ozone*, edited by C. S. Zerefos and A. Ghazi, p. 201, D. Reidel, Hingham, Mass., 1985.

Nicolet, M., On the molecular scattering in the terrestrial atmosphere: an empirical formula for its calculation in the homosphere, *Planet. Space Sci.*, *32*, 1467, 1984.

Norton, R. B., and J. F. Noxon, Dependence of stratospheric NO_3 upon latitude and season, *J. Geophys. Res.*, *91*, 5323, 1986.

Noxon, J. F., R. B. Norton, and W. R. Henderson, Observation of atmospheric NO_3, *Geophys. Res. Lett.*, *5*, 675, 1978.

Noxon, J. F., R. B. Norton, and E. Marovich, NO_3 in the troposphere, *Geophys. Res. Lett.*, *7*, 125, 1980.

Offermann, D., Some results from the MAP/GLOBUS 1983 campaign, *Ann. Geophys.*, *5A*, 187, 1987.

Pirre, M., R. Ramaroson, J. P. Naudet, and P. Rigaud, Altitude distribution of stratospheric NO_3, 2, Comparison of observations with model, *J. Geophys. Res.*, this issue.

Platt, U., D. Perner, J. Schroder, C. Kessler, and A. Toennissen, The diurnal variation of NO_3, *J. Geophys. Res.*, *86*, 11,965, 1981.

Pommereau, J. P., et al., Intercomparison of stratospheric NO_2 and NO_3 measurements during MAP/GLOBUS 1983, *Planet. Space Sci.*, *32*, 615, 1987.

Ravishankara, A. R., and R. L. Mauldin III, Temperature dependence of the NO_3 cross section in the 662-nm region, *J. Geophys. Res.*, *91*, 8709, 1986.

Ravishankara, A. R., and P. H. Wine, Absorption cross sections for NO_3 between 565 and 673 nm, *Chem. Phys. Lett.*, *101*, 73, 1983.

Rigaud, P., J. P. Naudet, and D. Huguenin, Simultaneous measurements of vertical distributions of stratospheric NO_3 and O_3 at different periods of the night, *J. Geophys. Res.*, *88*, 1463, 1983.

Rosen, J. M., and D. J. Hofmann, Optical modeling of stratospheric aerosols: Present status, *Appl. Opt.*, *25*, 410, 1986.

Sander, S. P., Temperature dependence of the NO_3 absorption spectrum, *J. Phys. Chem.*, *90*, 4135, 1986.

Sanders, R. W., S. Solomon, G. H. Mount, M. W. Bates, and A. L. Schmeltekopf, Visible spectroscopy at McMurdo Station, Antarctica, 3, Observations of NO_3, *Geophys. Res.*, *92*, 8339, 1987.

Simon, P. C., W. Peetermans, E. Plateau, P. Rigaud, J. P. Naudet, D. Huguenin, D. Offermann, and H. Rippel, Remote sensing ozone measurements from stratospheric balloon during the MAP/GLOBUS campaign 1983, *Planet. Space Sci.*, *35*, 595, 1987.

Twomey, S., Comparison of constrained linear inversion and an iterative nonlinear algorithm applied to indirect estimation of particle size distributions, *J. Comput. Phys.*, *18*, 188, 1975.

Vigroux, E., Contribution à l'étude expérimentale de l'absorption par l'ozone, *Ann. Phys.*, *8*, 709, 1953.

Werner, J., K. W. Rothe, and H. Walther, Measurements of the ozone profile up to 50 km altitude by differential absorption laser radar, in *Atmospheric Ozone*, edited by C. S. Zerefos and A. Ghazi, p. 446, D. Reidel, Hingham, Mass., 1985.

World Meteorological Organization, The stratosphere 1981: Theory and measurements, *Rep. 11*, Geneva, Switzerland, 1981.

World Meteorological Organization, Atmospheric ozone 1985, *Rep. 16*, Geneva, Switzerland, 1985.

D. Huguenin, Observatoire de Genève, CH 1290, Sauverny, Switzerland.

J. P. Naudet, P. Rigaud, and M. Pirre, Laboratoire de Physique et Chemie de l'Environnement, CNRS, 3A, Avenue Recherche Scientifique, 45071 Orléans Cedex 2, France.

(Received May 10, 1988;
revised October 11, 1988;
accepted October 11, 1988.)